Journal of Advances in Modeling Earth Systems

RESEARCH ARTICLE
10.1029/2018MS001468

Improving Assimilation of Radiance Observations by Implementing Model Space Localization in an Ensemble Kalman Filter

Lili Lei[1], **Jeffrey S. Whitaker**[2], **and Craig Bishop**[3]

[1]Key Laboratory of Mesoscale Severe Weather, Ministry of Education, and School of Atmospheric Sciences, Nanjing University, Nanjing, China, [2]NOAA Earth System Research Laboratory, Boulder, CO, USA, [3]School of Earth Sciences and ARC Centre of Excellence for Climate Extremes, The University of Melbourne, Melbourne, Victoria, Australia

Key Points:
- A modulation approach has been adopted to implement model-space localization in an ensemble Kalman filter
- EnKF with model-space vertical localization performs better than observation-space localization
- A 960-member ensemble is sufficient to turn off the vertical localization and yields significant improvements than an 80-member ensemble

Correspondence to:
L. Lei,
lililei@nju.edu.cn

Citation:
Lei, L., Whitaker, J. S., & Bishop, C. (2018). Improving assimilation of radiance observations by implementing model space localization in an ensemble Kalman filter. *Journal of Advances in Modeling Earth Systems*, *10*, 3221–3232. https://doi.org/10.1029/2018MS001468

Received 11 AUG 2018
Accepted 27 NOV 2018
Accepted article online 30 NOV 2018
Published online 25 DEC 2018

Abstract Experiments using the National Oceanic and Atmospheric Administration Finite-Volume Cubed-Sphere Dynamical Core Global Forecasting System (FV3GFS) reveal that the four-dimensional ensemble-variational method (4DEnVAR) performs similarly to an ensemble Kalman filter (EnKF) when no radiance observations are assimilated, but 4DEnVAR is superior to an EnKF when radiance observations are assimilated. The hypothesis for the cause of the differences between 4DEnVAR and EnKF is the difference in vertical localization, since radiance observations are integral observations in the vertical and 4DEnVAR uses model space localization while the EnKF uses observation space localization. A modulation approach, which generates an expanded ensemble from the raw ensemble and eigenvectors of the localization matrix, has been adopted to implement model space localization in the operational National Oceanic and Atmospheric Administration EnKF. As constructed, the expanded ensemble is a square root of the vertically localized background error covariance matrix, so no explicit vertical localization is necessary during the EnKF update. The size of the expanded ensemble is proportional to the rank of the vertical localization matrix—for a vertical localization scale of 1.5 (3.0) scale heights, 12 (7) eigenvectors explain 96% of the variance of the localization matrix, so the expanded ensemble is 12 (7) times larger than the raw ensemble. Results from assimilating only radiance observations in the FV3GFS model confirm that EnKF with model-space vertical localization performs better than observation-space localization, and produces results similar to 4DEnVAR. Moreover, a 960-member ensemble is sufficient to turn off the vertical localization entirely and yields significant improvements comparing to an 80-member ensemble with model space localization.

1. Introduction

The current National Centers for Environmental Prediction operational Global Forecasting System utilizes a hybrid four-dimensional ensemble-variational (4DEnVAR) data assimilation system (Kleist & Ide, 2015; Wang & Lei, 2014). The high-resolution control forecast is updated by the 4DEnVAR with a combination of time-invariant static background error covariance (**B**) and flow-dependent **B** estimated from a lower resolution ensemble, while the ensemble is updated using an ensemble Kalman filter (EnKF; Shlyaeva & Whitaker, 2018). The 4DEnVAR without static **B** and dynamic constraints (e.g., the tangent-linear normal-mode constrain, TLNMC, Kleist, Parrish, Derber, Treadon, Errico, & Yang, 2009) solves the same equations as the EnKF and apart from algorithmic details should produce a very similar solution. However, we have found this to be true only when no satellite radiance observations are assimilated.

Using the new Finite-Volume Cubed-Sphere Dynamical Core (FV3; Harris & Lin, 2013) version of the National Centers for Environmental Prediction Global Forecasting System (scheduled to become operational in 2019), data assimilation experiments are performed at a reduced resolution of 75 km with 64 vertical levels. The 4DEnVAR and EnKF experiments assimilate the operationally used observations every 6 hr from 00 UTC 1 January 2016 to 00 UTC 6 February 2016, and the data between 00 UTC 6 January 2016 and 00 UTC 6 February 2016 are analyzed. The details of experiments are described in section 3. The globally averaged root-mean-square error relative to the wind, temperature, and relative humidity of the two experiments with assimilation of all observations but radiance data is shown in Figure 1. The two experiments are nearly identical, with similar results are obtained for the Northern Hemisphere (NH; 20–90°N), the Tropics (TR; 20°S to 20°N), and the Southern Hemisphere (SH; 90–20°S; figures are not shown). When including radiance observations, 4DEnVAR has advantages over EnKF, especially over the SH, as shown in Figure 2. We

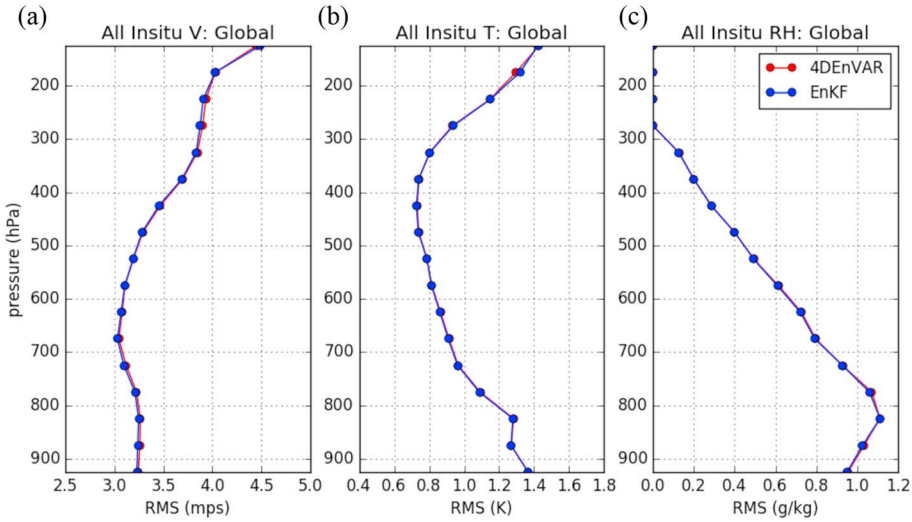

Figure 1. Globally and temporally averaged RMS background forecast observation innovation profiles that are the differences between 6-hr background forecasts interpolated to observation locations and in situ conventional observations including marine and land surface stations, rawinsonde, and aircraft between 00 UTC 6 January 2016 and 00 UTC 6 February 2016, for (a) wind, (b) temperature, and (c) relative humidity from experiments 4DEnVAR and ensemble Kalman filter assimilating conventional observations. 4DEnVAR = four-dimensional ensemble-variational method; EnKF = ensemble Kalman filter; RMS = root-mean-square; RH = relative humidity.

hypothesize that these differences are due to the way vertical localization is implemented in 4DEnVAR and the EnKF, since radiance observations are integral observations in the vertical and 4DEnVAR uses model space localization while the EnKF uses observation space localization.

The Kalman gain matrix (**K**) with model space localization (Houtekamer & Mitchell, 2001) can be written as

$$\mathbf{K}=\left(\rho_m \circ \mathbf{P}^f\right)\mathbf{H}^{\mathbf{T}}\left(\mathbf{H}\left(\rho_m \circ \mathbf{P}^f\right)\mathbf{H}^{\mathbf{T}}+\mathbf{R}\right)^{-1}, \tag{1}$$

where $\mathbf{P}^f$, a $k \times k$ matrix (k is number of state variables), is the sample background-error covariance matrix; **H**, a $p \times k$ matrix (p is number of observations), is the forward observation operator (linearized about the ensemble

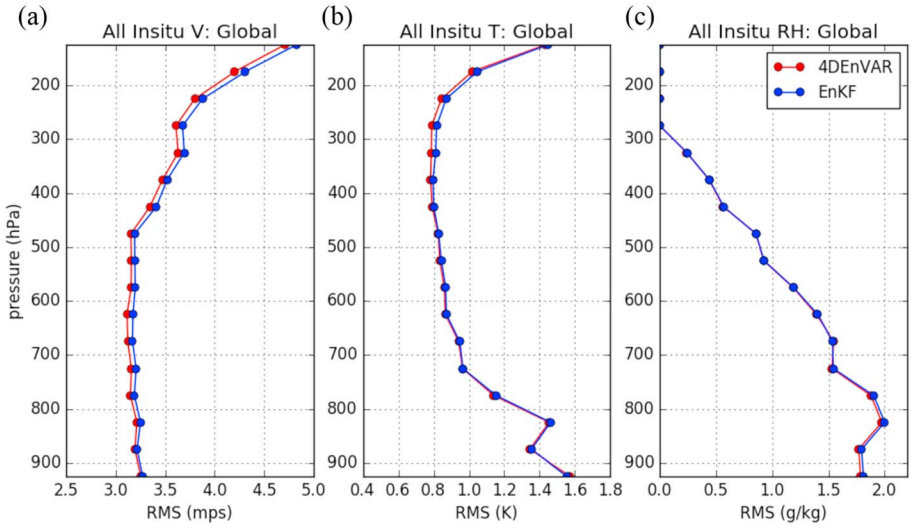

Figure 2. Same as in Figure 1 but for the Southern Hemisphere and experiments 4DEnVAR and EnKF assimilating both conventional and radiance observations. 4DEnVAR = four-dimensional ensemble-variational method; EnKF = ensemble Kalman filter; RMS = root-mean-square; RH = relative humidity.

mean background state); **R**, a $p \times p$ matrix, is the observation error covariance; ρ_m is the covariance localization matrix in model space; and $\circ$ denotes the Schur (element-wise) product. Localization in model space is directly applied to the background-error covariance matrix, and it is conducted before applying the forward observation operator. Thus, model space localization involves distances between state variables only. With localization in observation space, **K** can be written as

$$\mathbf{K}=\left(\rho_{o1}\circ\left(\mathbf{P}^f\mathbf{H}^\mathbf{T}\right)\right)\left(\rho_{o2}\circ\left(\mathbf{H}\mathbf{P}^f\mathbf{H}^\mathbf{T}\right)+\mathbf{R}\right)^{-1}, \tag{2}$$

where ρ_{o1} and ρ_{o2} are the localization matrices for observation space localization. The ρ_{o1} is an $k \times p$ matrix with each column containing localization function for one observation with the state vector, while ρ_{o2} is a $p \times p$ matrix with each column containing localization function for one observation with all the other observations. Localization in observation space is operated after the forward operator is applied to the background-error covariance matrix. Thus, observation space localization involves distances between observations and state variables and between observations with other observations. Model space localization (equation (1)) and observation space localization (equation (2)) are equivalent when **H** is local, but not equivalent when **H** is nonlocal as in the case of radiance observations (Campbell et al., 2010).

As nonlocal observations, satellite radiances can provide information about temperature, moisture, ozone, and other quantities in an atmospheric column. Therefore, the vertical structure of correlations between radiance observations and model state variables can be qualitatively different from those between local observations (i.e., the same quantities as model state variables) and model state variables (Anderson & Lei, 2013; Lei et al., 2016). Furthermore, the distance between a radiance observation and a model state variable is not well defined. For these reasons, vertical localization for radiance observations in observation space is not as straightforward as for local observations. Observation space localization is usually used in EnKF systems for reasons of computation efficiency. Radiance observations are often treated as local observations whose vertical locations are defined by the level at which the weighting function used in the radiative transfer peaks (e.g., Houtekamer & Mitchell, 2005; Houtekamer et al., 2005). In addition to the commonly used fixed Gaspari and Cohn localization (Gaspari & Cohn, 1999), there have been adaptive algorithms for localizing the impacts of radiance observations. Miyoshi and Sato (2007) used the flow-dependent normalized weighting function as vertical localization function. Lei et al. (2016) applied the global group filter (Lei & Anderson, 2014) to estimate the vertical localization function for satellite radiances. Fertig et al. (2007) updated the state at a given location by radiance observations that are strongly correlated to the model state. The potential imbalances caused by different types of localization were discussed by Greybush et al. (2011).

Besides the various adaptive localization algorithms for the radiance observations in observation space, Campbell et al. (2010) used the Navy Operational Global Atmospheric Prediction System and the Advanced Microwave Sounding Unit A (AMSU-A) observations to reveal that localizing radiance observations in model space was more accurate than localizing in observation space. However, motived by the AMSU-A observations assimilated by the Global Forecasting System and 4DEnVAR, Lei and Whitaker (2015) found that the opposite can be true when negative background error covariances occur with a predominately positive forward observation operator. In order to investigate the impact of observation space localization for radiances in the EnKF, and to validate the hypothesis that the observed differences between 4DEnVAR and EnKF when radiances are assimilated are due to vertical localization, a method for applying model space vertical localization in the EnKF is desired.

Bishop and Hodyss (2009a, 2009b) proposed an adaptive localization algorithm, ensemble correlations raised to a power, to better capture flow-dependent error correlations. They used it in a variation of Hunt et al.'s (2007) local observation volume form of Bishop et al.'s (2001) ensemble transform Kalman filter (ETKF) known as the LETKF. To reduce the computational cost of ensemble correlations raised to a power, a modulation matrix product between the raw ensemble perturbations and the eigenvectors of the localization matrix (equations 1 and 2 in Bishop & Hodyss 2009b) was used. This modulation process increases the number of ensemble perturbations in a way that implicitly imbeds the model space localization in the modulated ensemble covariance matrix. Modulated ensemble perturbations can be used in any type of EnKF update without localization to update the analysis mean. However, as noted in Bishop et al. (2017), modulated ensembles present a conundrum for EnKFs that create analysis perturbations by right-multiplying forecast perturbations by a transformation matrix (e.g., Bishop et al., 2001, ETKF; Hunt et al., 2007, local form of it).

Specifically, if not adjusted such EnKFs create the same number of analysis perturbations as the number of modulated forecast perturbations, which is much larger than the number of ensemble members needed to initialize the ensemble forecasting system. Thus, one is left with the problem of efficiently finding an analysis ensemble with fewer members whose covariance most accurately approximates the true analysis error covariance matrix. This conundrum does not arise in EnKFs whose analysis perturbations are created by left-multiplying the forecast perturbations by a matrix (e.g., Anderson, 2001; Houtekamer & Mitchell, 1998; Whitaker & Hamill, 2002). They escape this conundrum by left-multiplying the raw unmodulated ensemble perturbations by a transformation matrix to obtain an analysis ensemble with precisely the same number of analysis perturbations as forecast perturbations. To solve the conundrum for ETKF-like schemes, Bishop et al. (2017) derived a gain form of the ETKF that uses a left-multiplying transformation matrix rather than a right-multiplying transformation matrix and which includes an inherent localization-dependent inflation factor. This *Gain* form of the ETKF (the GETKF) provided precisely the same number of analysis perturbations as forecast perturbations, and the inherent localization-dependent inflation factor also improved its performance in idealized models. Among other things, this paper provides the first test of a local form of the GETKF (LGETKF) in a research version of an operational weather forecasting system. However, since the primary focus of the study is to quantify the effect of using modulated ensembles to implement model space localization in the vertical, the inherent inflation factor is set to unity in this study.

This paper is organized as follows. The methodology of implementing model space localization in a serial EnKF and a LGETKF is described in section 2. Section 3 discusses the experimental design. Results are presented in sections 4 and 5, and the findings of this study are summarized in section 6.

2. Methodology

National Oceanic and Atmospheric Administration (NOAA) has developed implementations of Whitaker and Hamill's (2002) ensemble square root filter (EnSRF) in a form that serially assimilates observations and the local form of Bishop et al.'s (2001) ETKF (Hunt et al., 2007) that assimilates all observations within an observation volume in a single step. The manner in which the larger-size ensemble of modulated ensemble perturbations should be used to update the ensemble mean and the smaller size ensemble of states to be propagated by the nonlinear model depends on the type of EnKF implemented and is an area of active research. In the following, we first introduce the modulation process and then discuss the methods by which modulated ensembles are incorporated within the EnSRF and LETKF separately.

Let $\boldsymbol{X} = \left[\mathbf{x}_1^{f\prime}, \mathbf{x}_2^{f\prime}, \ldots, \mathbf{x}_N^{f\prime}\right]/\sqrt{N-1}$, where $\mathbf{x}_j^{f\prime} = \mathbf{x}_j^f - \frac{1}{N}\sum_{i=1}^{N}\mathbf{x}_i^f$ is the jth ensemble perturbation corresponding to the jth ensemble forecast member $\mathbf{x}_j^f$ and $\boldsymbol{X}$ gives the square root of the sample background-error covariance matrix $\mathbf{P}^f = \boldsymbol{X}\boldsymbol{X}^T$. Let $\boldsymbol{W} = [\mathbf{w}_1, \mathbf{w}_2, \ldots, \mathbf{w}_L]$ give the square root of a model space localization matrix $\rho_m = \boldsymbol{W}\boldsymbol{W}^T$. As proven in equations 1 and 2 of Bishop and Hodyss (2009b), the sample background-error covariance matrix with model space localization can be given by the factorization property:

$$\mathbf{P}_{loc}^f = \rho_m \circ \mathbf{P}^f = \left(\boldsymbol{W}\boldsymbol{W}^T\right)\circ\left(\boldsymbol{X}\boldsymbol{X}^T\right) = \boldsymbol{Z}\boldsymbol{Z}^T, \tag{3}$$

where $\boldsymbol{Z} = \boldsymbol{W}\Delta\boldsymbol{X}$ and Δ denote the modulation product. If $\boldsymbol{X}$ has N (ensemble size) columns and $\boldsymbol{W}$ has L (eigenvectors of ρ_m) columns, the modulated ensemble perturbations are defined by

$$\boldsymbol{Z} = \frac{1}{\sqrt{N-1}}\left[\left[\mathbf{x}_1^{f\prime}\circ\mathbf{w}_1, \mathbf{x}_2^{f\prime}\circ\mathbf{w}_1, \ldots, \mathbf{x}_N^{f\prime}\circ\mathbf{w}_1\right], \left[\mathbf{x}_1^{f\prime}\circ\mathbf{w}_2, \mathbf{x}_2^{f\prime}\circ\mathbf{w}_2, \ldots, \mathbf{x}_N^{f\prime}\circ\mathbf{w}_2\right], \ldots, \left[\mathbf{x}_1^{f\prime}\circ\mathbf{w}_L, \mathbf{x}_2^{f\prime}\circ\mathbf{w}_L, \ldots, \mathbf{x}_N^{f\prime}\circ\mathbf{w}_L\right]\right] \tag{4}$$

The modulated ensemble perturbations involve an expansion of ensemble size from N to $M = NL$. The mean of the modulated ensemble perturbations is equal to zero since $\frac{1}{M}\sum_{i=1}^{M}\mathbf{z}_i^{f\prime} = \sum_{k=1}^{L}\sum_{j=1}^{N}\frac{1}{\sqrt{N-1}}\mathbf{x}_j^{f\prime}\circ\mathbf{w}_k = \sum_{k=1}^{L}\left(\sum_{j=1}^{N}\frac{1}{\sqrt{N-1}}\mathbf{x}_j^{f\prime}\right)\circ\mathbf{w}_k = 0$. Thus, adding the ensemble mean to the modulated ensemble perturbations gives the modulated ensemble

$$\mathbf{z}_i^f = \frac{1}{N}\sum_{j=1}^{N}\mathbf{x}_j^f + \sqrt{M}\mathbf{z}_i^{f\prime}. \tag{5}$$

The modulated ensemble has the same ensemble mean as the raw ensemble and the same covariance as the *localized* ensemble covariance matrix.

2.1. Use of Modulated Ensemble in EnSRF

The EnSRF uses the traditional Kalman gain to update the ensemble mean and a reduced Kalman gain to update the ensemble perturbations. Using the modulated ensemble perturbations, the update equation for the ensemble mean is

$$\begin{aligned}\overline{\mathbf{x}}^a &= \overline{\mathbf{x}}^f + \boldsymbol{Z}(\mathbf{HZ})^{\mathbf{T}}\left((\mathbf{HZ})(\mathbf{HZ})^{\mathbf{T}} + \mathbf{R}\right)^{-1}\left[\mathbf{y} - \overline{H(\mathbf{x}^f)}\right] \\ &= \overline{\mathbf{x}}^f + \mathbf{P}_{\mathrm{loc}}^f\mathbf{H}^{\mathbf{T}}\left(\mathbf{H}\mathbf{P}_{\mathrm{loc}}^f\mathbf{H}^{\mathbf{T}} + \mathbf{R}\right)^{-1}\left[\mathbf{y} - \overline{H(\mathbf{x}^f)}\right],\end{aligned} \tag{6}$$

and the update equation for the ensemble perturbations is

$$\begin{aligned}\mathbf{x}'^a &= \mathbf{x}'^f - \boldsymbol{Z}(\mathbf{HZ})^{\mathbf{T}}\left[\left(\sqrt{(\mathbf{HZ})(\mathbf{HZ})^{\mathbf{T}} + \mathbf{R}}\right)^{-1}\right]^T\left[\sqrt{\left((\mathbf{HZ})(\mathbf{HZ})^{\mathbf{T}} + \mathbf{R}\right)} + \sqrt{\mathbf{R}}\right]^{-1}\mathbf{H}\mathbf{x}'^f \\ &= \mathbf{x}'^f - \mathbf{P}_{\mathrm{loc}}^f\mathbf{H}^{\mathbf{T}}\left[\left(\sqrt{\mathbf{H}\mathbf{P}_{\mathrm{loc}}^f\mathbf{H}^{\mathbf{T}} + \mathbf{R}}\right)^{-1}\right]^T\left[\sqrt{(\mathbf{H}\mathbf{P}_{\mathrm{loc}}^f\mathbf{H}^{\mathbf{T}} + \mathbf{R})} + \sqrt{\mathbf{R}}\right]^{-1}\mathbf{H}\mathbf{x}'^f\end{aligned} \tag{7}$$

It is evident that the traditional Kalman gain $\mathbf{K} = \boldsymbol{Z}(\mathbf{HZ})^{\mathbf{T}}((\mathbf{HZ})(\mathbf{HZ})^{\mathbf{T}} + \mathbf{R})^{-1}$ and reduced Kalman gain $\widetilde{\mathbf{K}} = \boldsymbol{Z}(\mathbf{HZ})^{\mathbf{T}}\left[\left(\sqrt{(\mathbf{HZ})(\mathbf{HZ})^{\mathbf{T}} + \mathbf{R}}\right)^{-1}\right]^T\left[\sqrt{\left((\mathbf{HZ})(\mathbf{HZ})^{\mathbf{T}} + \mathbf{R}\right)} + \sqrt{\mathbf{R}}\right]^{-1}$ are matrices with dimension $k \times p$ (k and p are numbers of state variables and observations), so that it is straightforward to use $\mathbf{K}$ and $\widetilde{\mathbf{K}}$ for updating the raw ensemble mean and perturbations. Since $\mathbf{P}_{\mathrm{loc}}^f = (\mathbf{HZ})(\mathbf{HZ})^{\mathbf{T}}$ is equivalent to $\rho_m \circ \mathbf{P}^f$, the ensemble analysis from equations (6) and (7) is equivalent to that with model space localization (equation (1)).

2.2. Use of Modulated Ensembles in a Local Observation Volume Framework

To better accommodate ensemble expansions such as that which results from ensemble modulation, Bishop et al. (2017) proposed a gain form of the ensemble transform Kalman filter (GETKF) that could be used in the local observation volume framework of a LETKF as a local GETKF or LGETKF.

Let $\widetilde{H}\boldsymbol{Z} = \frac{1}{\sqrt{M}}\mathbf{R}^{-1/2}\left[\left(H(\mathbf{z}_1^f) - \overline{H(\mathbf{z}^f)}\right), \left(H(\mathbf{z}_2^f) - \overline{H(\mathbf{z}^f)}\right), \ldots, \left(H(\mathbf{z}_M^f) - \overline{H(\mathbf{z}^f)}\right)\right]$, where $\overline{H(\mathbf{z}^f)} = \frac{1}{M}\sum_{i=1}^{M}H(\mathbf{z}_i^f)$. Using singular value decomposition (SVD), $\widetilde{H}\boldsymbol{Z}$ can be written as

$$\widetilde{H}\boldsymbol{Z} = \mathbf{E}\Gamma^{1/2}\mathbf{C}^T. \tag{8}$$

Equations 11 and 12 from Bishop et al. (2017) give the usual ETKF or LETKF update equation of ensemble mean:

$$\overline{\mathbf{x}}^a = \overline{\mathbf{x}}^f + \boldsymbol{Z}\mathbf{C}(\Gamma + \mathbf{I})^{-1}\mathbf{C}^T\left(\widetilde{H}\boldsymbol{Z}\right)^T\mathbf{R}^{-1/2}\left[\mathbf{y} - \overline{H(\mathbf{x}^f)}\right], \tag{9}$$

while equation 29 from Bishop et al. (2017) implies that the update equation for the ensemble perturbations is

$$\mathbf{X}^{a\prime} = a\left\{\mathbf{X}^{f\prime} - \boldsymbol{Z}\mathbf{C}\left[\mathbf{I} - (\Gamma + \mathbf{I})^{-1/2}\right]\Gamma^{-1}\mathbf{C}^T\left(\widetilde{H}\boldsymbol{Z}\right)^T\widetilde{H}\mathbf{X}^{f\prime}\right\}, \tag{10}$$

where $\widetilde{H}\mathbf{X}^{f\prime} = \mathbf{R}^{-1/2}\left[\left(H(\mathbf{x}_1^f) - \overline{H(\mathbf{x}^f)}\right), \left(H(\mathbf{x}_2^f) - \overline{H(\mathbf{x}^f)}\right), \ldots, \left(H(\mathbf{x}_N^f) - \overline{H(\mathbf{x}^f)}\right)\right]$ and a is an inflation factor that in Bishop et al. (2017) was used to ensure a consistency relation between the posterior modulated ensemble and the posterior raw ensemble. In this work, we set $a = 1$. Unlike the ETKF, which would update all the M modulated ensemble perturbations, equation (10) just updates the raw N-member forecast

ensemble. The updated N ensemble perturbations and the ensemble mean posterior are then used to initialize the next ensemble background forecast. In the appendix, as in Bishop et al. (2001), we emphasize that when the number of observations p in an observation volume exceeds the number of modulated ensemble members M, it will, in general, be more computationally efficient to obtain $\mathbf{C}$ and Γ from a direct eigenvalue decomposition of $\left(\widetilde{H}\boldsymbol{Z}\right)^T\widetilde{H}\boldsymbol{Z}$ rather than from a direct SVD of $\widetilde{H}\boldsymbol{Z}$. It is often more computationally efficient to implement equation (10) as a series of operations on $\widetilde{H}\mathbf{X}^{f'}$ rather than as the operation of a modified gain matrix on $\mathbf{X}^{f'}$.

3. Experimental Design

The Finite-Volume Cubed-Sphere Dynamical Core–Global Forecasting System (FV3GFS; https://vlab.ncep.noaa.gov/web/fv3gfs), scheduled to become operational at NOAA in 2019, is used for assimilation experiments of EnKF and 4DEnVAR at a reduced resolution of 75-km resolution and 64 vertical levels. The default ensemble size N is 80. The operationally assimilated observations include conventional observations (http://www.emc.ncep.noaa.gov/mmb/data_processing/prepbufr.doc/table_2.htm), GPS radio occultation bending angle, and satellite radiances (http://www.emc.ncep.noaa.gov/mmb/data_processing/prepbufr.doc/table_18.htm). Experiments discussed in section 1 assimilate either conventional observations and GPS radio occultation bending angle observations (Figure 1) or both conventional observations, GPS radio occultation bending angle, and satellite radiances (Figure 2). To clearly examine the impact of model space and observation space localizations on the assimilation of radiance observations, experiments in sections 4 and 5 only assimilate satellite radiances. The gridpoint statistical interpolation (Kleist, Parrish, Derber, Treadon, Wu, & Lord, 2009; Wu et al., 2002) is used to compute and save the values of $\mathbf{H}\mathbf{x}^f$ for the ensemble mean, along with the linearized $\mathbf{H}$ operator. The linearized $\mathbf{H}$ operator is used in the EnKF to compute the observation-space ensemble perturbations as described by Shlyaeva and Whitaker (2018). The bias correction coefficients for the satellite radiance bias correction are provided by a separate 4DEnVar experiment using the same forecast model run at 50-km resolution but assimilating both conventional and radiance observations. The observation error variance ($\mathbf{R}$; which is assumed diagonal) follows the operational values.

To remove spurious covariances arising from sampling errors, covariance localization is used. By assuming that covariance localization is separable, the localization is applied separately in the horizontal and vertical. The GC localization function is used for both horizontal and vertical localization, and the horizontal (vertical) localization tapers the observation impact to 0 at 1,500 km (1.5 scale heights). EnKF experiments of serial EnSRF (LETKF) use these GC localization length scales that taper the observation impact (inverse of the observation error variance) to 0, but experiment 4DEnVAR incorporates Gaussian e-folding scale for localization, and the equivalent horizontal (vertical) localization in Gaussian e-folding scale is approximately 581 km (0.581 scale heights). The same localization parameters are used for experiments with model space and observation space localizations. A doubled vertical localization length scale (3.0 scale heights) is used in an additional experiment. To maintain appropriate ensemble spread and avoid filter divergence, multiplicative covariance inflation is used. The relaxation-to-prior spread (Whitaker & Hamill, 2012) that relaxes posterior ensemble spread back to prior ensemble spread with a relaxation coefficient of 0.85 is applied. Stochastic parameterizations, such as the Stochastically Perturbed Parameterization Tendencies Scheme (Palmer et al., 2009), Stochastic Kinetic Energy Backscatter (Palmer et al., 2009), and Perturbed Boundary Layer Humidity (Tompkins & Berner, 2008), are used to represent model uncertainty within the ensemble forecast step, and no additive inflation is applied.

To assimilate the observations, experiment 4DEnVAR uses the National Centers for Environmental Prediction hybrid 4DEnVAR (Kleist & Ide, 2015; Wang & Lei, 2014), in which the prior ensemble mean is updated by the 4DEnVAR and the ensemble perturbations are updated by the NOAA EnKF (NCAR Developmental Testbed Center, 2015; Shlyaeva & Whitaker, 2018). In the single-resolution configuration, there is no separate control forecast—instead, the ensemble mean prior is used as background for the hybrid 4DEnVAR analysis, which is different from the dual-resolution configuration used in operations. The 4DEnVAR utilizes 4-D prior ensemble perturbations and no static $\mathbf{B}$ component, a single outer loop, and has the TLNMC (Kleist, Parrish, Derber, Treadon, Errico, & Yang, 2009) turned off to facilitate direct comparisons with the EnKF. Experiment EnKF uses the NOAA EnKF to update both the prior ensemble mean and ensemble perturbations. Although the same

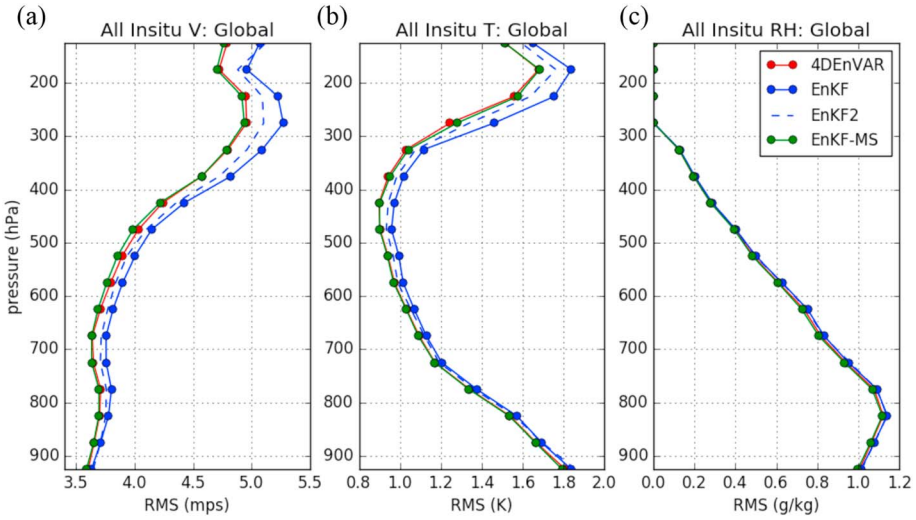

Figure 3. Same as in Figure 1 but for experiments 4DEnVAR, EnKF, EnKF2 (with doubled vertical localization length scale), and EnKF-MS assimilating only radiance observations. 4DEnVAR = four-dimensional ensemble-variational method; EnKF = ensemble Kalman filter RH = relative humidity; RMS = root-mean-square.

horizontal and vertical localization length scales are used for experiments 4DEnVAR and EnKF, experiment 4DEnVAR utilizes model space localization, and experiment EnKF applies observation space localization. The LETKF algorithm (Hunt et al., 2007) of the NOAA EnKF is used to compute analysis increments with observation-space localization.

Experiment EnKF-MS is the same as experiment EnKF, except that vertical localization is performed in model space using the modulated ensemble approach with the LGETKF algorithm described in section 2. Since radiance observations are integral observations in the vertical, here only the vertical localization is performed in model space, while the horizontal localization is still performed in observation space. The vertical GC localization matrix is truncated to retain L eigenvectors that explain more than 95% of the variance. For the FV3GFS model with a GC vertical localization function with length scale of 1.5 scale heights, $L = 12$ explains 96% of the variance, and gives a 960 ($M = NL$) member modulated ensemble. Each eigenvector has a length equal to the number of model vertical levels (64 in this case). To generate the modulated ensemble, an element-wise product of each localization eigenvector with every model state column for each of the three-dimensional state variables (e.g., temperature, humidity, and zonal and meridional winds) is performed, and the first element of each eigenvector multiplies each element of the two-dimensional state variables like surface pressure. The M modulated ensemble priors (equations (4) and (5)) instead of the N raw ensemble priors are ingested by the NOAA EnKF. During the assimilation process, vertical localization is turned off, because the modulated ensemble already contains the vertical localization in model space. The raw ensemble mean and raw ensemble perturbations are updated using equations (9) and (10).

The assimilation experiments extend from 00 UTC 1 January 2016 to 00 UTC 6 February 2016. Observations are assimilated every 6 hr, and 3-hr background forecasts are used for the forward operator. The first five days of assimilation are discarded to avoid transient effects, and the remaining data between 00 UTC 6 January 2016 and 00 UTC 6 February 2016 are used for verification. The 6-hr background forecasts are interpolated to observation locations of wind, temperature, and relative humidity and compared to the in situ conventional observations that include marine and land surface stations, rawinsonde, and aircraft. The RMS observation innovations are averaged globally (GL), in the Northern Hemisphere (NH; 20–90°N), the Tropics (TR; 20°S to 20°N), and the Southern Hemisphere (SH; 90–20°S), respectively. The temporally averaged RMS observation innovation profiles will be presented.

4. Results

The globally and temporally averaged RMS observation innovations profiles for wind, temperature, and relative humidity from experiments assimilating only radiance observations are shown in Figure 3. Figure 4

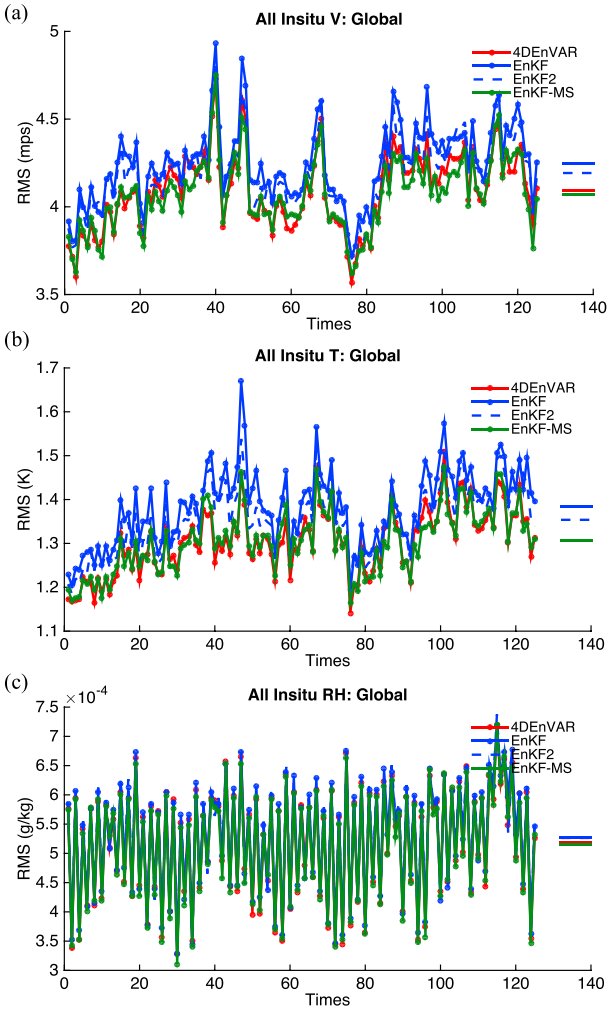

Figure 4. Time series of the globally and vertically averaged RMS background forecast observation innovations for (a) wind, (b) temperature, and (c) relative humidity of experiments 4DEnVAR, EnKF, EnKF2 (with doubled vertical localization length scale), and EnKF-MS assimilating only radiance observations. The right-side bars denote temporal mean of the error. 4DEnVAR = four-dimensional ensemble-variational method; EnKF = ensemble Kalman filter; RH = relative humidity; RMS = root-mean-square.

displays the time series of the globally and vertically averaged RMS background forecast observation innovations, and the right-side bars denote temporal mean of the error. Similar results are obtained for the NH, TP, and SH (figures are not shown).

Model space localization (experiment 4DEnVAR) has advantages over observation space localization (experiment EnKF), and the advantages are enlarged with assimilation of only radiance observations, which are shown by comparing Figure 3 to Figure 2. A Student's *t* test is used to assess the significance of the globally, vertically, and temporally averaged RMS error differences. The differences between experiment 4DEnVAR and EnKF for wind and temperature are significant given a 95% confidence, while the differences for relative humidity are insignificant.

Experiment EnKF-MS performs nearly the same as experiment 4DEnVAR. The differences between experiment EnKF-MS and 4DEnVAR are not significant for all variables. If the serial EnSRF is used instead of the LGETKF, nearly identical results are obtained (not shown). This demonstrates that the modulated ensemble approach can be used to perform model space localization for both the serial EnSRF and LETKF algorithms.

Lei et al. (2016) showed that a broader localization length scale was favored for assimilating the Advanced Microwave Sounding Unit-A (AMSU-A) radiance observations with observation space localization. Thus, an additional experiment with doubled vertical localization length scale for observation space localization (experiment EnKF2) is performed. Experiment EnKF2 has smaller errors than experiment EnKF, but it still has larger errors than EnKF-MS. The differences between experiment EnKF2 and EnKF-MS for wind and temperature are significant given a 95% confidence, but not for the differences of relative humidity.

Given the FV3GFS model with 75-km resolution and 64 vertical levels, assimilating only radiance observations, an ensemble size of 80 and 12 eigenvectors for the vertical localization matrix, the cost of computing the analysis increment using model space localization (experiment EnKF-MS) is about twice the cost of computing the analysis increment with observation-space localization (experiment EnKF). However, if the localization length scale is doubled, only seven eigenvectors of the vertical localization matrix are required to explain 96% of the variance, and EnKF-MS is nearly twice as fast as the EnKF with observation space localization. This is because the cost savings associated with only having to compute the LGETKF eigenanalysis once for each model column dominates the extra cost associated with the increased ensemble size as the localization length scale increases (and the size of the modulated ensemble decreases). For our configuration, the cross-over point where EnKF-MS (LGETKF) becomes faster than EnKF (LETKF) occurs for vertical localization length scales between 2 and 2.5 scale heights. Further details regarding the efficient implementation of model-space localization in the LGETKF are included in the appendix.

5. Turning Off Vertical Localization

In sections 3 and 4, the vertical GC localization matrix of the FV3GFS model with a localization length scale of 1.5 scale heights is truncated to retain the L (L = 12) eigenvectors that explain 96% of the variance, which gives a 960 ($M = NL$) modulated ensemble. This suggests that a 960-member forecast background ensemble should be large enough to turn off the vertical localization entirely. To demonstrate this hypothesis, an experiment LETKF960 is performed. Experiment LETKF960 is the same as experiment EnKF except that vertical localization is turned off and background forecast ensemble size is increased by a factor of 12 from 80 to

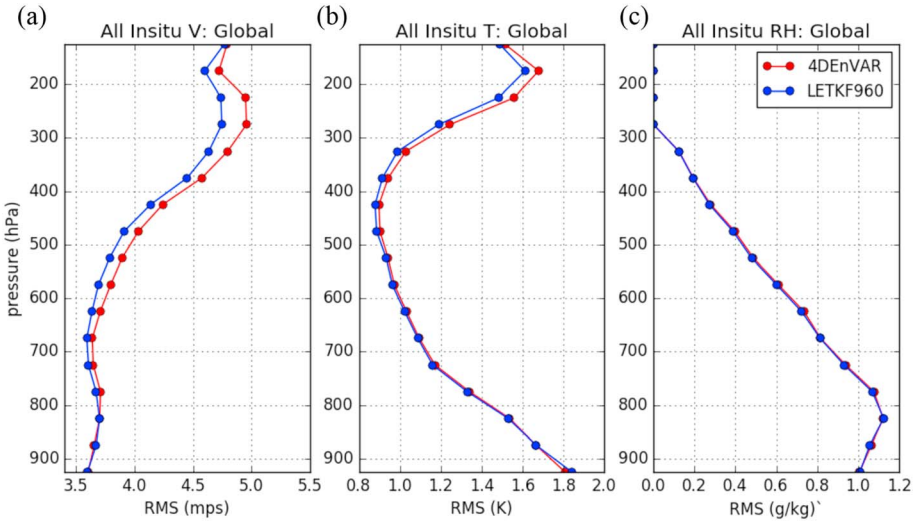

Figure 5. Same as in Figure 3 but for experiments 4DEnVAR and LETKF9604DEnVAR = four-dimensional ensemble-variational method; EnKF = ensemble Kalman filter.

960. No changes were made to the horizontal localization or inflation parameters, although a broader horizontal localization and less inflation may be preferred with a larger ensemble size.

The globally and temporally averaged RMS observation innovations profiles for experiments LETKF960 and previous 4DEnVAR with 80 members are shown in Figure 5, and similar results are also obtained for the NH, TP, and SH (figures are not shown). The increase of ensemble size to 960 and elimination of vertical localization lead to significant improvement comparing to an 80-member ensemble with model space localization. This suggests that there is still significant room for improvement in the operational system by reducing or mitigating the effects of sampling error, even in the presence of model error. Similar results would be expected from a 4DEnVAR experiment with 960 members to experiment LETKF960, since vertical localization can be turned off given a 960-member ensemble. Although experiment LETKF960 requires more computational resources to advance 960 ensemble members than experiments with the default 80 members, its performance is superior to experiment 4DEnVAR with 80 ensemble members and experiments EnKF-MS and EnKF-LGETKF with 960 modulated ensemble members. The extra cost of the LETKF960 experiment is dominated by the twelvefold increase in the cost of running the background ensemble forecast. Arguably, the increased cost associated with a larger background ensemble is easier to accommodate in an operational environment, since this cost is incurred in a less time critical part of the data assimilation cycle and is perfectly scalable.

6. Discussions and Conclusions

Using the FV3GFS model at 75-km resolution, a 4DEnVAR experiment without static **B** and TLNMC performs nearly identically to an EnKF experiment when no radiance observations are assimilated. However, 4DEnVAR is superior when satellite radiances are assimilated. It is hypothesized that the cause of the differences between 4DEnVAR and the EnKF is primarily due to differences in vertical localization, since radiance observations are integral observations in the vertical and 4DEnVAR uses model space localization while EnKF uses observation space localization.

To demonstrate the hypothesis, a method for performing model space localization in an ensemble Kalman filter was implemented using a modulation approach (Bishop & Hodyss, 2009b). The modulation approach generates the modulated ensemble from the model-integrated raw ensemble and eigenvectors of the localization matrix. The modulated ensemble implicitly contains model space localization. For an EnSRF, it is straightforward to apply the modulated ensemble to compute the Kalman gain and reduced Kalman gain, and then apply these to update the original "raw" ensemble. To apply the modulation approach in an LETKF, the gain form of the local ensemble transform Kalman filter (LGETKF; Bishop et al., 2017) is used. The trade-off is increased computational cost for the EnKF, because the modulated ensemble has a L times

larger ensemble size than the raw ensemble, where L is the number of eigenvectors of the localization matrix. However, for the LGETKF, this additional cost can be offset by cost savings associated with the need to only compute the singular value decomposition in equation (8) once for each model column (instead of for every model grid point). In fact, if the vertical localization length scale is large enough (and L is small enough), model-space localization can be more efficient than observation-space localization.

The performance of the modulated ensemble with ensemble Kalman filters is examined using the FV3GFS model assimilating only radiance observations. The vertical GC localization with length scale of 1.5 scale heights is truncated to retain 12 eigenvectors that explain 96% of the variance. Thus, given a default raw ensemble size of 80, the modulated ensemble has size of 960. The LGETKF with model-space vertical localization produces results similar to 4DEnVAR. Thus, the ability of the modulation approach to perform model space localization for ensemble Kalman filters is demonstrated, and the hypothesis that the difference between model space localization and observation space localization is the primary cause of the performance difference observed between 4DEnVAR and EnKF is confirmed. Moreover, the performance of ensemble Kalman filters assimilating radiance observations has been improved by use of the model-space localization via a modulation approach.

Since 12 eigenvectors of the vertical GC localization matrix explain 96% of the variance, this suggests that a 960-member ensemble may be sufficient to turn off the vertical localization entirely. An experiment using the LETKF with 960 ensemble members and no vertical localization yielded significant improvements comparing to an 80-member ensemble with model space localization, indicating that there is still significant room for improvement by reducing sampling error, even in an operational system with significant model error. The extra computational cost of the LETKF960 experiment is dominated by the background ensemble forecast step—which is perfectly scalable and occurs at a less time-critical period in an operational environment (just before new observations become available).

Although model space localization can improve the assimilation of radiance observations for ensemble Kalman filters and can be implemented using the modulation approach, there can be a significant increase in computational cost for small vertical localization length scales. An alternative method for performing model-space localization in the serial EnSRF is to utilize the linearized forward operator to allow the localization to occur in model space before application of the forward operator (A. Shlyaeva, personal communication, 2018). Although this method is more expensive for the localization scales used here, it should be less expensive for sufficiently small localization length scales since it becomes less computationally expensive as localization scales decrease. An alternative method to improve the assimilation of radiance observations in an EnKF is through the use of an empirical localization function (Lei et al., 2016). A detailed comparison between the empirical localization function and model space localization for radiance assimilation will be presented in a future study.

Localization was demonstrated to be the primary reason for the different results between (nonhybrid) 4DEnVAR and EnKF, but other factors (such as the use of a static component in the background-error covariance, the TLNMC, the use of "outer loops" to account for nonlinearities in the forward operator, and the fact that whereas 4DEnVar's global solve allows all observations to contribute to the analysis at a single location, in the (LETKF) EnKF only observations within the local observation volume of the analysis point can contribute to the analysis) could also contribute when the EnKF is compared with the full operational hybrid system. The contribution of these other factors to differences between hybrid 4DEnVAR and EnKF will be the subject of further investigation.

Appendix A: Computational Considerations for Implementation of LGETKF Equations (8)–(10)

Although equation (8) expresses the complete singular value decomposition (SVD) of a *pxM* matrix, note that the LGETKF equations for updating the ensemble mean (9) and perturbations (10) only require the singular values listed in the diagonal matrix $\Gamma^{1/2}$ and the right orthonormal singular vectors $\mathbf{C}$. Hence, as noted by Bishop et al. (2001), when the number of observations p (in a local observation volume) exceeds the number of modulated ensemble members M the SVD problem of diagonalizing the MxM matrix $\left(\widetilde{H}\boldsymbol{Z}\right)^T\widetilde{H}\boldsymbol{Z}=\mathbf{C}\Gamma\mathbf{C}^T$ involves fewer operations than the problem of diagonalizing the pxM matrix $\widetilde{H}\boldsymbol{Z}$.

For equation (10), let k be the number of variables in the vertical column to be updated by the LGETKF. One then has the choice of either (i) explicitly computing the kxp modified gain matrix $\widetilde{\mathbf{K}}=\boldsymbol{Z}\mathbf{C}\left[\mathbf{I}-(\Gamma+\mathbf{I})^{-1/2}\right]\Gamma^{-1}\mathbf{C}^{T}\left(\widetilde{H}\boldsymbol{Z}\right)^{T}$ and then operating on each of the column vectors of $\widetilde{H}\mathbf{X}^{f'}$ or (ii) implementing a series of operations whose effect is equivalent to $\widetilde{\mathbf{K}}$.

For option (i), assuming that $p > M > k > N$, the most expensive operation in the formation of $\widetilde{\mathbf{K}}$ is the product of the matrices in curly brackets $\left\{\boldsymbol{Z}\mathbf{C}\left[\mathbf{I}-(\Gamma+\mathbf{I})^{-1/2}\right]\Gamma^{-1}\right\}\left\{\left[\left(\widetilde{H}\boldsymbol{Z}\right)^{T}\right]\right\}$. Evaluating this term involves order kMp operations. Once $\widetilde{\mathbf{K}}$ has been formed, evaluating $\widetilde{\mathbf{K}}\left(\widetilde{H}\mathbf{X}^{f'}\right)$ requires a relatively inexpensive order kpN operations. For option (ii) one can order the operations either from right to left or from left to right. Let the lower index on the embedded curly brackets in the following expressions indicate the sequence of operations, then

$$\text{Right-to-left sequence}:\equiv\left\{\boldsymbol{Z}\left\{\mathbf{C}\left\{\left[\mathbf{I}-(\Gamma+\mathbf{I})^{-1/2}\right]\Gamma^{-1}\left\{\mathbf{C}^{T}\left\{\left(\widetilde{H}\boldsymbol{Z}\right)^{T}\left(\widetilde{H}\mathbf{X}^{f'}\right)\right\}_{1}\right\}_{2}\right\}_{3}\right\}_{4}\right\}_{5}.$$

$$\text{Left-to-right sequence}:\equiv\left\{\left\{\left\{\left\{\{\boldsymbol{Z}\mathbf{C}\}_{1}\left[\mathbf{I}-(\Gamma+\mathbf{I})^{-1/2}\right]\Gamma^{-1}\right\}_{2}\mathbf{C}^{T}\right\}_{3}\left(\widetilde{H}\boldsymbol{Z}\right)^{T}\right\}_{4}\left(\widetilde{H}\mathbf{X}^{f'}\right)\right\}_{5}$$

The orders of the number of operations associated with the matrix operations in the right to left sequence are MpN, M^2N, MN, M^2N, and kMN, respectively. The most expensive step in this right to left sequence is the MpN operations associated with the first step. For the left to right sequence, the orders are kM^2, kM, kM^2, kMp, and kpN, respectively. The most expensive step in this left to right sequence is the penultimate step with order kMp operations. Note that this order is the same as the order of the number of operations associated with the most expensive step of option (i)'s explicit formation of the modified gain matrix. Hence, the most expensive step of the right to left sequence is k/N times faster than the most expensive steps of both the left to right sequence approach and the explicit formation of gain approach.

To reveal the actual computational implications in an atmospheric data assimilation scheme of this simple analysis, the LGETKF was implemented in NOAA's system in two different ways: by explicitly computing the modified gain as in option (i) and also by implementing the right-to-left sequence of operations of option (ii). It was found that the right-to-left sequence of operations implementation was 4–5 times faster than the explicit formation of gain approach.

Acknowledgments
Thanks to two anonymous reviewers for their constructive suggestions. This work is jointly sponsored by the National Key R&D Program of China through grant 2017YFC1501603, the National Natural Science Foundation of China through grant 41675052, the NOAA High-Impact Weather Prediction Project (HIWPP) under award NA14OAR4830123, and the NOAA/NWS Next-Generation Global Prediction System (NGGPS) project. Craig H. Bishop acknowledges support from the Australian Research Council's Centres of Excellence Scheme (CE170100023). The data used to generate the simulation experiments were obtained from the National Centers for Environmental Prediction (NCEP; https://www.ncdc.noaa.gov/data-access/model-data/model-datasets/global-forcast-system-gfs).

References

Anderson, J. L. (2001). An ensemble adjustment Kalman filter for data assimilation. *Monthly Weather Review*, *129*(12), 2884–2903. https://doi.org/10.1175/1520-0493(2001)129<2884:AEAKFF>2.0.CO;2

Anderson, J. L., & Lei, L. (2013). Empirical localization of observation impact in ensemble Kalman filters. *Monthly Weather Review*, *141*(11), 4140–4153. https://doi.org/10.1175/MWR-D-12-00330.1

Bishop, C., Etherton, B., & Majumdar, S. (2001). Adaptive sampling with the ensemble transform Kalman filter. Part I: The theoretical aspects. *Monthly Weather Review*, *129*(3), 420–436. https://doi.org/10.1175/1520-0493(2001)129<0420:ASWTET>2.0.CO;2

Bishop, C. H., & Hodyss, D. (2009a). Ensemble covariances adaptively localized with ECO-RAP. Part 1: Tests on simple error models. *Tellus Series A: Dynamic Meteorology and Oceanography*, *61*, 84–96.

Bishop, C. H., & Hodyss, D. (2009b). Ensemble covariances adaptively localized with ECO-RAP. Part 2: A strategy for the atmosphere. *Tellus Series A: Dynamic Meteorology and Oceanography*, *61*, 97–111.

Bishop, C. H., Whitaker, J. S., & Lei, L. (2017). Gain form of the ensemble transform Kalman filter and its relevance to satellite data assimilation with model space ensemble covariance localization. *Monthly Weather Review*, *145*(11), 4575–4592. https://doi.org/10.1175/MWR-D-17-0102.1

Campbell, W. F., Bishop, C. H., & Hodyss, D. (2010). Vertical covariance localization for satellite radiances in ensemble Kalman filters. *Monthly Weather Review*, *138*(1), 282–290. https://doi.org/10.1175/2009MWR3017.1

Fertig, E. J., Hunt, B. R., Ott, E., & Szunyogh, I. (2007). Assimilating non-local observations with a local ensemble Kalman filter. *Tellus Series A: Dynamic Meteorology and Oceanography*, *59*, 719–730.

Gaspari, G., & Cohn, S. E. (1999). Construction of correlation functions in two and three dimensions. *Quarterly Journal of the Royal Meteorological Society*, *125*(554), 723–757. https://doi.org/10.1002/qj.49712555417

Greybush, S. J., Kalnay, E., Miyoshi, T., Ide, K., & Hunt, B. R. (2011). Balance and ensemble Kalman filter localization techniques. *Monthly Weather Review*, *139*(2), 511–522. https://doi.org/10.1175/2010MWR3328.1

Harris, L. M., & Lin, S.-J. (2013). A two-way nested global-regional dynamical core on the cubed-sphere grid. *Monthly Weather Review*, *141*(1), 283–306. https://doi.org/10.1175/MWR-D-11-00201.1

Houtekamer, P. L., & Mitchell, H. L. (1998). Data assimilation using an ensemble Kalman filter technique. *Monthly Weather Review*, *126*(3), 796–811. https://doi.org/10.1175/1520-0493(1998)126<0796:DAUAEK>2.0.CO;2

Houtekamer, P. L., & Mitchell, H. L. (2001). A sequential ensemble Kalman filter for atmospheric data assimilation. *Monthly Weather Review*, *129*(1), 123–137. https://doi.org/10.1175/1520-0493(2001)129<0123:ASEKFF>2.0.CO;2

Houtekamer, P. L., & Mitchell, H. L. (2005). Ensemble Kalman filtering. *Quarterly Journal of the Royal Meteorological Society*, *131*(613), 3269–3289. https://doi.org/10.1256/qj.05.135

Houtekamer, P. L., Mitchell, H. L., Pellerin, G., Buehner, M., Charron, M., Spacek, L., & Hansen, B. (2005). Atmospheric data assimilation with the ensemble Kalman filter: Results with real observations. *Monthly Weather Review*, *133*(3), 604–620. https://doi.org/10.1175/MWR-2864.1

Hunt, B. R., Kostelich, E. J., & Szunyogh, I. (2007). Efficient data assimilation for spatiotemporal chaos: A local ensemble transform Kalman filter. *Physica D: Nonlinear Phenomena*, *230*(1-2), 112–126. https://doi.org/10.1016/j.physd.2006.11.008

Kleist, D. T., & Ide, K. (2015). An OSSE-based evaluation of hybrid variational–ensemble data assimilation for the NCEP GFS. Part II: 4DEnVAR and hybrid variants. *Monthly Weather Review*, *143*(2), 452–470. https://doi.org/10.1175/MWR-D-13-00350.1

Kleist, D. T., Parrish, D. F., Derber, J. C., Treadon, R., Errico, R. M., & Yang, R. (2009). Improving incremental balance in the GSI 3DVAR analysis system. *Monthly Weather Review*, *137*(3), 1046–1060. https://doi.org/10.1175/2008MWR2623.1

Kleist, D. T., Parrish, D. F., Derber, J. C., Treadon, R., Wu, W., & Lord, S. (2009). Introduction of the GSI into NCEP global data assimilation system. *Weather Forecasting*, *24*(6), 1691–1705. https://doi.org/10.1175/2009WAF2222201.1

Lei, L., & Anderson, J. L. (2014). Comparisons of empirical localization techniques for ensemble Kalman filters in a simple atmospheric general circulation model. *Monthly Weather Review*, *142*(2), 739–754. https://doi.org/10.1175/MWR-D-13-00152.1

Lei, L., Anderson, J. L., & Whitaker, J. S. (2016). Localizing the impact of satellite radiance observations using a global group ensemble filter. *Journal of Advances in Modeling Earth Systems*, *8*, 719–734. https://doi.org/10.1002/2016MS0000627

Lei, L., & Whitaker, J. S. (2015). Model space localization is not always better than observation space localization for assimilation of satellite radiances. *Monthly Weather Review*, *143*(10), 3948–3955. https://doi.org/10.1175/MWR-D-14-00413.1

Miyoshi, T., & Sato, Y. (2007). Assimilating satellite radiances with local ensemble transform Kalman filter (LETKF) applied to the JMA global model (GSM). *Scientific Online Letters on the Atmosphere*, *3*, 37–40. https://doi.org/10.2151/sola.2007-010

NCAR Developmental Testbed Center (2015). NOAA ensemble Kalman filter (beta release v1.0 compatible with GSI community release v3.3) user's guide. NCAR (55 pp). Retrieved from http://www.dtcenter.org/com-GSI/users/docs/enkf_users_guide/EnKF_UserGuide_v1.0Beta.pdf

Palmer, T. N., R. Buizza, F. Doblas-Reyes, T. Jung, M. Leutbecher, G. J. Shutts, M. Steinheimer, et al., 2009: Stochastic parameterization and model uncertainty. ECMWF Tech. Memo. 598 (44 pp). Retrieved from http://www.ecmwf.int/sites/default/files/elibrary/2009/11577-stochastic-parametrization-and-model-uncertainty.pdf

Shlyaeva, A., & Whitaker, J. S. (2018). Using the linearized observation operator to calculate observation-space ensemble perturbations in ensemble filters. *Journal of Advances in Modeling Earth Systems*, *10*, 1414–1420. https://doi.org/10.1029/2018MS001309

Tompkins, A. M., & Berner, J. (2008). A stochastic convective approach to account for model uncertainty due to unresolved humidity variability. *Journal of Geophysical Research*, *113*, D18101. https://doi.org/10.1029/2007JD009284

Wang, X., & Lei, T. (2014). GSI-based four-dimensional ensemble–variational (4DEnsVar) data assimilation: Formulation and single-resolution experiments with real data for NCEP Global Forecast System. *Monthly Weather Review*, *142*(9), 3303–3325. https://doi.org/10.1175/MWR-D-13-00303.1

Whitaker, J. S., & Hamill, T. M. (2002). Ensemble data assimilation without perturbed observations. *Monthly Weather Review*, *130*(7), 1913–1924. https://doi.org/10.1175/1520-0493(2002)130<1913:EDAWPO>2.0.CO;2

Whitaker, J. S., & Hamill, T. M. (2012). Evaluating methods to account for system errors in ensemble data assimilation. *Monthly Weather Review*, *140*(9), 3078–3089. https://doi.org/10.1175/MWR-D-11-00276.1

Wu, W. S., Purser, R. J., & Parrish, D. F. (2002). Three-dimensional variational analysis with spatially inhomogeneous covariances. *Monthly Weather Review*, *130*(12), 2905–2916. https://doi.org/10.1175/1520-0493(2002)130<2905:TDVAWS>2.0.CO;2